ELSEVIER

Polymer 42 (2001) 2555–2567

polymer

www.elsevier.nl/locate/polymer

Volume and enthalpy recovery of polystyrene

S.L. Simon[a,*], J.W. Sobieski[b], D.J. Plazek[c]

[a]*Chemical Engineering Department, Texas Tech University, Lubbock, TX 79409, USA*
[b]*Chemical Engineering Department, University of Pittsburgh, Pittsburgh, PA 15261, USA*
[c]*Materials Science and Engineering Department, University of Pittsburgh, Pittsburgh, PA 15261, USA*

Received 13 March 2000; received in revised form 17 August 2000; accepted 17 August 2000

Abstract

Volume and enthalpy recovery measurements were used to study the physical aging behavior of a polystyrene. Isothermal aging at temperatures near T_g was studied with aging times ranging from several minutes to several days. The data are satisfactorily fit using the Tool–Narayanswamy–Moynihan model of structural recovery. The times required to reach equilibrium are the same for the two properties at temperatures where equilibrium was achieved. Extrapolation to lower temperatures using the model indicates that the times required to reach equilibrium may be different for the two properties at these lower temperatures. The recovery data were plotted as the departure from equilibrium and then were shifted horizontally to superpose at long times. The shift factors for volume and enthalpy recovery data agree with one another above 94°C but they diverge below this temperature. The shift factor data deviates from the WLF or VTFH equation for temperatures below T_g. In addition, we find that the normalized rate of approach is the same for volume and enthalpy recovery at 97°C in the limit of a linear temperature jump, but it differs between the two properties for a nonlinear jump even though the times required to reach equilibrium are the same.

Keywords: Physical aging; Polystyrene; Volume and enthalpy recovery

1. Introduction

Glasses, including polymeric glasses, are inherently nonequilibrium materials. Hence, their physical and mechanical properties change with time as the glass attempts to reach equilibrium through changes on the molecular scale. This behavior is often referred to in the literature as structural recovery or physical aging, and several reviews [1–10] have been written.

We are interested in understanding the interrelationship of properties during physical aging in order to ultimately predict material behavior with limited experimental data. There are a number of reports in the literature on the time scales of evolution for different properties in amorphous polymeric materials but there seems to be no universal agreement [11–24]. A discussion session at a recent international meeting [25] addressed this issue.

We suggest that some of the apparent contradiction in the literature may come from comparison of the kinetics of recovery for various properties rather than comparison of the times required to reach equilibrium. For example, from our polyetherimide data [11,12], the time required to reach equilibrium for volume, enthalpy, and creep appeared to be the same within experimental error, whereas the rate of approach to equilibrium differed. However, there are data in the literature that suggest that properties are not coupled as we suggest and that the times to reach equilibrium for different properties may not be the same [13–22]. To further investigate this issue, in this work we present volume and enthalpy recovery data for polystyrene, a material studied by several groups of researchers [13–16,23].

The work previously performed on polystyrene is similar to much of the work in the literature in that it appears at first glance to be contradictory. Oleinik reported a constant relationship between enthalpy and volume during structural recovery with dH/dV being $1–2 \times 10^9$ J/m^3 for down-jump experiments over the entire measurement time interval and for all aging temperatures [23]. Adachi and Kotaka, on the other hand, reported differences in the kinetics of volume and enthalpy recovery; they report that after a double temperature jump in which the "memory" effect [2] is observed, the time to reach the maximum in volume was longer than the time to reach the maximum in enthalpy [13]. Weitz and Wunderlich also reported differences in the kinetics of volume and enthalpy recovery for their experiments which involved cooling under pressure and observing structural recovery after the pressure was released; they

* Corresponding author. Tel.: +1-806-780-1763; fax: +1-806-742-3552.
E-mail address: sindee.simon@coe.ttu.edu (S.L. Simon).

0032-3861/01/$ - see front matter
PII: S0032-3861(00)00623-6

report that at 70°C, the major enthalpy recovery process started only after the initial volume recovery process was over [14]. Roe and Millman measured enthalpy recovery and the evolution of room temperature creep curves and reported that the enthalpy reached equilibrium much faster than did the creep compliance [15]. Petrie also measured the changes in storage modulus and logarithmic decrement and compared them to enthalpy recovery but reported that the changes in the mechanical behavior corresponded to the changes in the enthalpy, although the figures show that the mechanical properties stop evolving somewhat earlier than the enthalpy [16]. As already mentioned, in addition to these works on the relative time scales for polystyrene, other researchers [17–22] have reported different time scales for different properties on materials other than polystyrene, and the results are similarly not universal.

Structural recovery data can be modeled using Moynihan's formulation [26] of the Tool–Narayanaswamy [27,28] model of structural recovery (TNM model). The model is equivalent to that developed by Kovacs, et al. [29] (KAHR model). Both models account for the nonlinearity and the nonexponentiality of the recovery process. The evolution of the departure from equilibrium, δ, during isothermal aging is represented by the generalized Kohlrausch–William–Watts (KWW) [30,31] function:

$$\delta = \delta_0 \exp\left\{-\left(\int_0^t \frac{\mathrm{d}t}{\tau_0}\right)^{\beta}\right\} \tag{1}$$

where for volume recovery $\delta = \delta_v = (v(t) - v_\infty)/(v_\infty)$, $v(t)$ is the time-dependent volume, v_∞ is the volume at equilibrium, and δ_0 is the value of the departure from equilibrium initially (immediately after jumping up or down to the aging temperature); for enthalpy, $\delta = \delta_h = \Delta H_\infty - \Delta H_a(t)$, where $\Delta H_a(t)$ is the change in enthalpy after aging for some time t and ΔH_∞ is the total change in enthalpy found in reaching equilibrium. The departure from equilibrium is a relative value for volume (being dimensionless) but this is not the case for enthalpy due to the fact that there is not an absolute scale for enthalpy.

The nonexponentiality of structural recovery is accounted for in the TNM model by the parameter β. The nonlinearity is incorporated by allowing τ to be a function of temperature and fictive temperature, T_f, the latter of which was first used by Tool [28] to quantify the structure of a glass:

$$\ln \tau_0 = \ln A + \frac{x\Delta h}{\mathrm{R}T} + \frac{(1-x)\Delta h}{\mathrm{R}T_f} \tag{2}$$

where $ln\,A$, x, and $\Delta h/\mathrm{R}$ are generally taken to be fitting parameters. The nonlinearity parameter x partitions the structure (T_f) and temperature dependence of the relaxation time [26]. The fictive temperature is defined as the temperature at which a material would reach equilibrium if heated (or cooled) along the glass line. Hence, at equilibrium, the fictive temperature is equal to the temperature. Given the narrow temperature range used in this work, the Arrhenius temperature dependence of the equilibrium relaxation times given by Eq. (2) is a valid approximation to the observed WLF (Williams–Landell–Ferry) [32] behavior. We note that the dependence of the characteristic relaxation time on temperature and fictive temperature is an arbitrary choice. According to free volume theory, free volume (which can be written in terms of temperature and fictive temperature) should be the dependent variable [32].

To solve Eqs. (1) and (2), the relationship between T_f and the departure from equilibrium must be written:

$$T_f = T_a + \frac{\delta_v}{\Delta\alpha} \qquad \text{for volume} \tag{3}$$

$$T_f = T_a + \frac{\delta_h}{\Delta C_p} \qquad \text{for enthalpy} \tag{4}$$

where T_a is the isothermal aging temperature, $\Delta\alpha$ is the change in the thermal expansion coefficient $(1/v)(\mathrm{d}v/\mathrm{d}T)$ at the glass temperature, and ΔC_p is the change in the heat capacity at the glass temperature. We note that Eqs. (3) and (4) can also be used to relate δ_0, the initial departure from equilibrium in Eq. (1), to the initial fictive temperature, T_{f0}.

Eqs. (1) and (2), coupled with either (3) or (4), can be solved numerically to describe the change in volume or enthalpy as a function of time during isothermal aging. The equations can also be modified using Boltzmann superposition [33] to describe the relaxation during more complicated thermal histories, including cooling or heating legs [26,29,34,35], and sinusoidal temperature modulation [36,37]. For cooling at a finite rate from above T_g to the aging temperature, the structural recovery response is calculated as the sum of the responses to small step changes simulating the cooling [26]. In addition to a constant rate of cooling, the temperature history for a real sample during cooling to T_a can be modeled using the general heat conduction equation:

$$\frac{\mathrm{d}T}{\mathrm{d}t} = c(T_a - T) \tag{5}$$

where c is the heat transfer coefficient and T_a is the aging temperature.

2. Methodology

2.1. Material

The material studied is a polystyrene (PS), Dylene 8 from Arco Polymers. The sample has a number-average molecular weight of 92,800 g/mol, a weight-average molecular weight of 221,000 g/mol, and a z-average molecular weight of 423,000 g/mol.

2.2. Dilatometric studies

A traditional capillary dilatometer using mercury as the

surrounding fluid was used for the volume recovery measurements. A 4 g cylindrical sample was vacuum molded. Holes were drilled axially and radially to decrease thermal lag. Temperature jump experiments were accomplished by placing the dilatometer in a bath maintained at 104°C until thermal equilibrium was reached (several minutes) and then quickly transferring the dilatometer to a bath maintained at the aging temperature to ±0.02°C. The time for temperature equilibration (±0.1°C) was found to be approximately 100 s. Time zero for the physical aging experiment is taken as the time at which the bath transfer was initiated. There is some controversy surrounding whether time zero should be taken after completion of the quench [12], midway through the quench [38], or at the start of the quench [39]. The reason for taking time zero midway through or at the beginning of the quench is to attempt to correct the data for the finite temperature jump since the recovery that occurs during cooling would take longer at the aging temperature [40]. Modeling work has shown that for the cooling history in the dilatometric experiments, taking time zero at the beginning of finite quench results in insignificant error in data on a logarithmic time scale compared to the results of a perfect quench for times greater than approximately two times the thermal equilibration time [41]. However, in this work, we actually modeled the quench itself for the dilatometric experiments.

The thermocouples used to monitor the temperature of the oil baths were calibrated using a platinum resistance thermometer (PRT), itself calibrated using the National Bureau of Standards (now, the National Institute of Standards and Technology) temperature scale by Leeds and Northrup. Maintenance of the calibration is periodically checked with ice point readings. The absolute temperature is considered to be accurate to 0.01°C.

2.3. DSC studies

A Perkin–Elmer DSC-7 differential scanning calorimetry was used for the measurement of enthalpy recovery after isothermal physical aging. A single 10.59 mg polystyrene sample, sealed in an aluminum pan, was used for all of the DSC data. To erase any previous thermal history, the sample was heated to above T_g (to 130°C) for several minutes. The sample was then cooled at 30°C/min to the isothermal aging temperature and aged for a predetermined time of aging (t_a) ranging from 5 min to 3 days. After isothermal aging, the sample was cooled at 30°C/min to 40°C, and data were subsequently collected during a heating ramp from 40 to 130°C at 10°C/min. To obtain an accurate baseline for analyzing the enthalpy recovery data, the sample was then cooled to 40°C at 30°C/min and "unaged" data are subsequently collected by immediately heating at 10°C/min. The cooling leg after isothermal aging was necessary in order to insure good temperature control over the temperature range in which the recovery occurs.

The change in enthalpy during physical aging, ΔH_a, can be determined by the difference in the areas under the aged and the unaged scans, respectively [16]. To this end, both curves are integrated between temperatures where the curves overlap, one temperature below and one above the aging peak. The procedure assumes that the same degree of relaxation occurs during cooling for both the aged and unaged glasses. Due to the relatively high rates of cooling used in the DSC experiments, this assumption is expected to be valid. We note that since the two heating scans, one of aged material and the other for unaged material, were obtained one after another, there is expected to be no affect of instrument baseline drift on ΔH_a. Even so, we used a custom-designed ethylene glycol refrigerator cooling system maintained at 5°C, which was near or above the dew point temperature, in order to minimize frost build-up and/or water condensation on the DSC heat sink in order to insure a stable and reproducible baseline.

The temperature and heat flow of the DSC were calibrated on heating at 10°C/min using gallium, indium, and a liquid crystal standard, (+)-4-*n*-hexyloxyphenyl-4′-(2′-methylbutyl)-biphenyl-4-carboxylate [42] (CE-3 from T.M. Leslie, University of Alabama; smectic to cholesteric transition at 78.8°C). No correction was made for thermal lag, which is on the order of 1°C for a heating rate of 10°C/min [43], because although thermal lag will affect the shape and placement of the enthalpy recovery peak [35], it will not affect the area of the peak.

To insure that the isothermal aging temperatures are correct, the temperature calibration obtained using the three standards was corrected by the difference between the melting point of indium at a rate of 0.1°C/min and that at 10°C/min. We use the 0.1°C/min calibration as the isothermal case because it gave the same results as the extrapolation of the results from several runs made at various rates to the isothermal condition, and the former requires less effort.

2.4. Model calculations

The best fit of the data to the Tool–Narayanaswamy–Moynihan model [26–28] was found by minimizing the sum of χ^2 for all aging temperatures with the data of each temperature being weighted equally in the sum. The Marquardt algorithm [44] was used to search the parameter space for the minimum. For volume recovery, the TNM equations in conjunction with the general heat equation was used to model both the quench from 104°C to the aging temperature and the isothermal recovery at the aging temperature. Hence, five parameters were fit: $\Delta h/R$, x, β, $\ln A$, and c (the latter being the heat transfer coefficient). The value of $\Delta\alpha$ was obtained from experimental data. For enthalpy recovery, a perfect quench was assumed due to the small sample size and high rates of cooling obtained in the DSC. Hence, four parameters were fit:

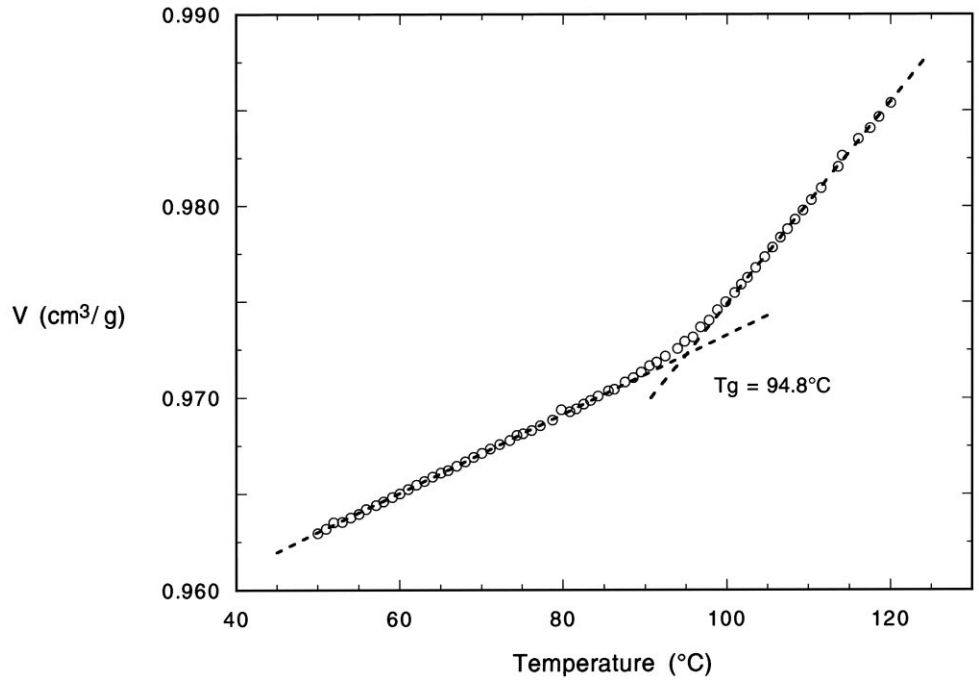

Fig. 1. Volume as a function of temperature obtained dilatometrically during cooling at 0.2°C/min.

Δh/R, x, β, $\ln A$; T_{f0} and ΔC_p were determined from the temperature dependence of ΔH_∞ using Eq. (4). Values of the parameters are given in Section 3.

3. Results and discussion

3.1. Cooling studies

The volume versus temperature cooling curve obtained at 0.2°C/min is shown in Fig. 1. The glass temperature is determined by the intersection of the extrapolated equilibrium and glassy lines, and is found to be 94.8°C. The thermal expansion coefficient $\alpha = 1/V(\mathrm{d}V/\mathrm{d}T)$ is found to be 5.5×10^{-4} and $2.1 \times 10^{-4}\ \mathrm{K}^{-1}$, in the equilibrium and glassy regions, respectively. These values agree with those of other researchers [45–49] as shown in Table 1.

3.2. Volume recovery

Volume recovery is shown in Fig. 2 for material aged at temperatures ranging from 88 to 100°C for times up to several days. The data is plotted as the relative departure from equilibrium, $\delta_v = (v(t) - v_\infty/v_\infty)$. The specific volume at equilibrium, v_∞, is determined experimentally by the value at which the volume levels off at long times for temperatures at which equilibrium is achieved. For the lower two temperatures, v_∞ is estimated by extrapolation of the equilibrium volume versus temperature line.

The relative departure from equilibrium decreases approximately linearly with the logarithm of increasing aging time and then levels off as equilibrium is approached. As the aging temperature decreases, the curves are shifted to longer times. Over the range of temperatures studied, the rate of structural recovery, $\mathrm{d}v/\mathrm{d}(\log t)$, is approximately $5 \times 10^{-4}\ \mathrm{cm}^3\ \mathrm{g}^{-1}$ per logarithmic decade of time independent of aging temperature in the range where the response is

Table 1
Thermal expansion coefficients reported for polystyrene

α_{liquid} ($10^4\ \mathrm{K}^{-1}$)	α_{glass} ($10^4\ \mathrm{K}^{-1}$)	$\Delta\alpha$ ($10^4\ \mathrm{K}^{-1}$)	Reference
5.4	2.0	3.4	Braun and Kovacs [45]
5.7	2.4	3.3	Greiner and Schwarzl [46]
4.9	1.6	3.3	Lee and McGarry [47]
5.5			Ueberreiter and Kanig [48]
		3.0	McKinney and Simha [49]
5.5	2.1	3.4	Present work

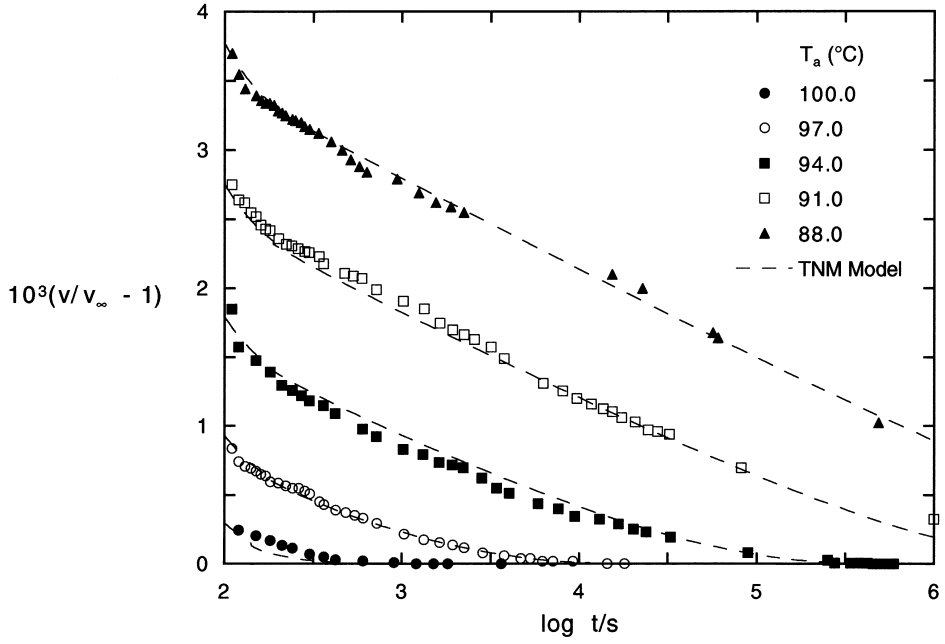

Fig. 2. Evolution of the relative departure from equilibrium for volume. Lines are the fit to the TNM model of structural recovery; model parameters are listed in Table 2.

linear with the logarithm of time. The rate we measure is somewhat lower than the rates reported by Adachi and Kotaka [13], which along with Kovacs data [2], were shown to follow a linear relationship as a function of molecular weight (M); for the molecular weight we studied, $dv/d(\log t)$ is predicted by their relationship to be 7×10^{-4} cm^3/g, somewhat higher than the value we observed. The apparent discrepancy arises from the fact that the rate of volume relaxation depends on the initial fictive temperature of the unaged glass, or in other words, on the temperature from which the glass-forming liquid is quenched. Kovacs showed that the higher the temperature from which the quench is made, the faster the rate of relaxation at short times, whereas at long times, the volume recovery curves approach one another and coincide [2]. In our work, the material is quenched from 104°C, whereas in the work by Adachi et al. and Kovacs, the material is quenched from 120 and 115°C, respectively. Hence, the rate of volume recovery

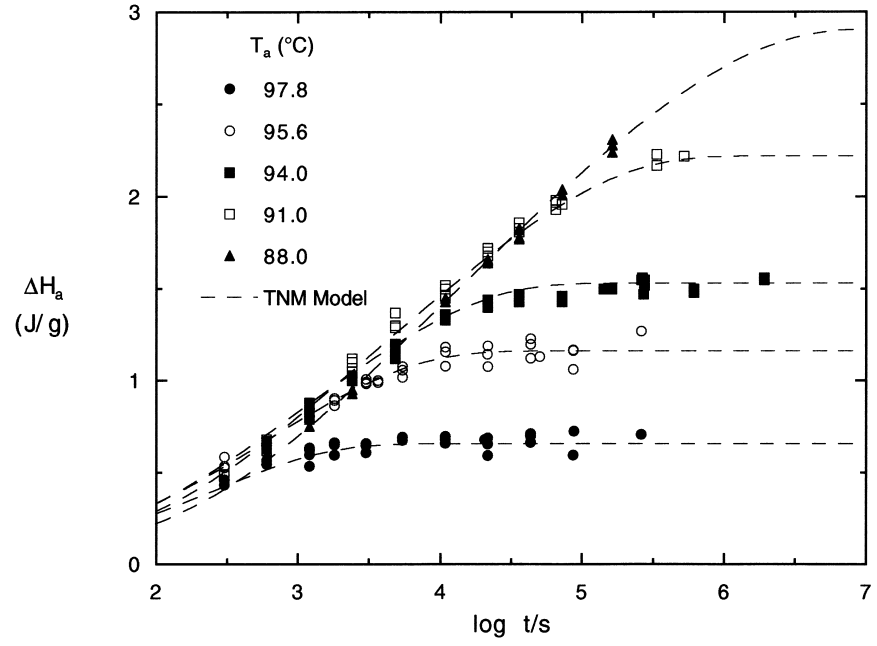

Fig. 3. Evolution of the change in enthalpy during aging. Lines are the fit to the TNM model of structural recovery; model parameters are listed in Table 2.

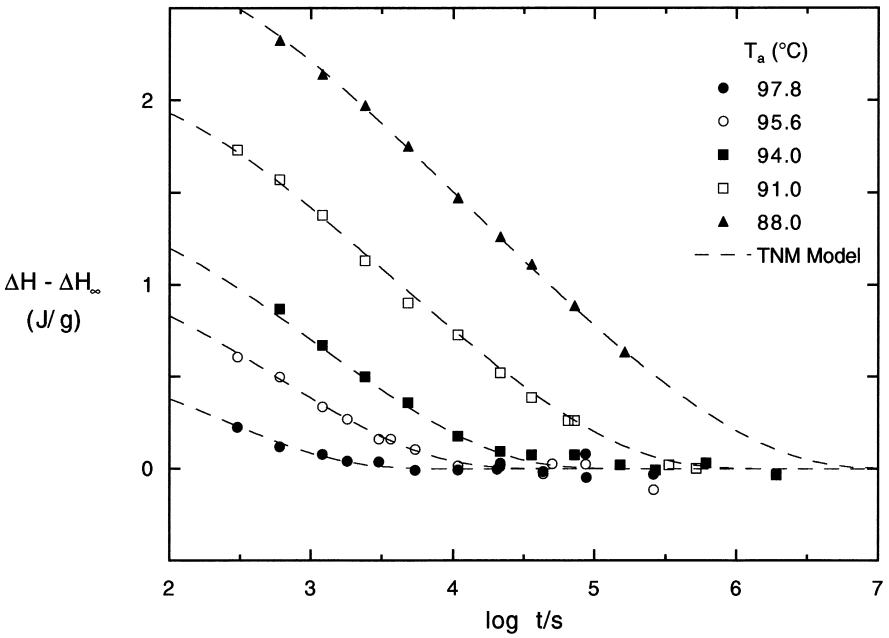

Fig. 4. Evolution of the relative departure from equilibrium for enthalpy; data points are averages. Lines are the fit to the TNM model of structural recovery; model parameters are listed in Table 2.

reported by the latter is faster than that reported by us. It must be emphasized that the initial fictive temperature will not affect the time required to reach equilibrium unless the time scale of cooling is comparable to the time to reach equilibrium [11].

Depicted in Fig. 2 is also the best fit of the Tool–Narayanaswamy–Moynihan model [26–28] to the data. The model gives a good description of the data. The best fit model parameters are shown in Table 2; the value of $\Delta\alpha$ is given in Table 1. The model parameters used to fit the isothermal volume recovery data differ from literature values [8] provided in the review by Hodge. However, the literature values were obtained from fitting DSC temperature scans, and hence, this is not necessarily unexpected. The value for the apparent activation energy, Δh/R, might be expected to be comparable, however, if the times to reach equilibrium were similar for the two properties. The fit of the data shown in Fig. 2 was obtained by minimization of the difference between the model calculation and the experimental points for all five temperatures at once, with each temperature being equally weighted in the fit. A unique set of parameters is obtained if one fits all five data sets simultaneously. However, since the volume recovery curve after a down-jump is simply a stretched exponential, each particular data set can be equally well fit with various sets of model parameters. This is obvious to researchers familiar with such fitting of data but must be kept in mind when comparing data in the literature. Complicating comparisons is also the fact that the model parameters appear to depend on thermal history [6,8,10,35,50–59] such that one set of parameters may not adequately describe experimental results over a wide range of thermal history.

Table 2
TNM model parameters used to model volume and enthalpy recovery data

Parameter	Volume	Enthalpy
ΔH/R (kK)	146.1	100.4
β	0.70	0.74
x	0.10	0.36
$\ln A$ (s^{-1})	−387.40	−264.25
T_{f0} (°C)	104.0	101.6[a]
$\Delta\alpha$ (kK^{-1})	0.34[b]	
ΔC_p ($J\,g^{-1}\,K^{-1}$)		0.21[a]
c (s^{-1})	0.0260	

[a] T_{f0} and ΔC_p for enthalpy were obtained from the values of ΔH_∞ at the temperatures where equilibrium was achieved.
[b] $\Delta\alpha$ was determined experimentally (see Table 1).

3.3. Enthalpy recovery

Enthalpy recovery is shown in Fig. 3 for material aged at temperatures ranging from 88.0 to 97.8°C for times from several minutes up to several days. Three data points were obtained at each aging time (except for the longest times where fewer points were obtained). The scatter in the data is similar to that of other researchers (better than ±0.1 J/g). The enthalpy behaves similarly to the volume, with the change in enthalpy increasing approximately linearly with the logarithm of the aging time and then leveling off at equilibrium.

The rate of enthalpy change, $d(\Delta H_a)/d \log t$, in the regime where it is approximately linear is 0.6 J/g per logarithmic decade of time. In comparison, the rate of enthalpy change in Roe and Millman's data [15] and in

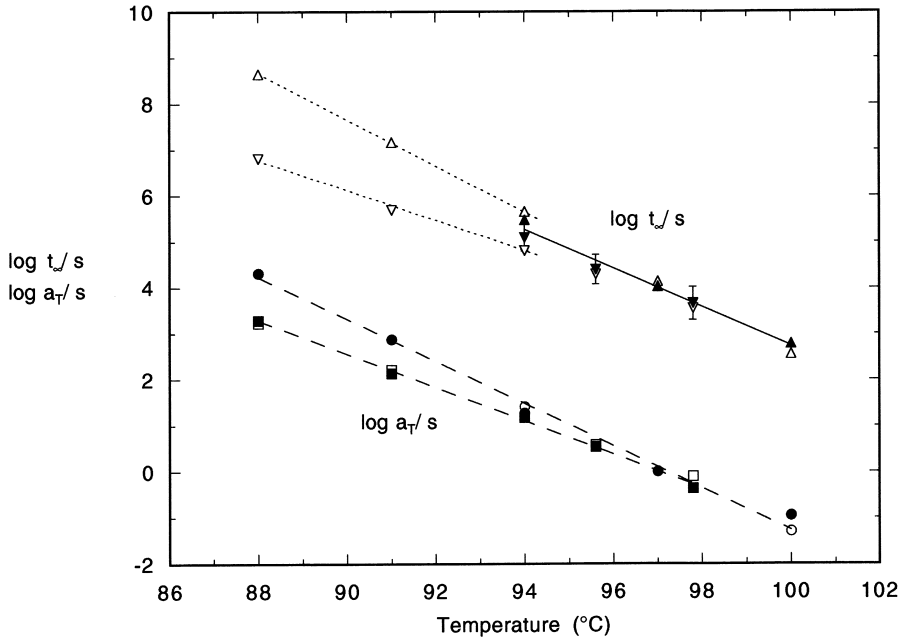

Fig. 5. Temperature dependence of the logarithm of the times required to reach equilibrium and of the shift factors for both the data (solid symbols) and the model calculations (open symbols). Triangles and circles: volume; inverted triangles and circles: enthalpy.

Petrie's work [16] is approximately 0.8 J/g per decade and 0.6 J/g per decade, respectively. Using our rate of enthalpy change, we obtain a value for the ratio of the change of enthalpy to that of volume, dH/dV, of 1.2×10^9 J/m^3 in the region where both properties vary logarithmically with time. This value is consistent with that reported by Oleinik [23].

The fit of the Tool–Narayanaswamy–Moynihan model [26–28] is also shown in Fig. 3. The model parameters used in the fit are shown in Table 2. The model was actually fit to the enthalpy data shown in Fig. 4 in terms of the enthalpic departure from equilibrium ($\Delta H_{a\infty} - \Delta H_a$) where the multiple data points obtained at each aging time are averaged. The enthalpy data was modeled as a perfect quench with an initial fictive temperature (T_{f0}) of 100.7°C for all the aging temperatures modeled due to the high rate of quench achievable in the DSC. The value of T_{f0} was determined from a linear fit of ΔH_∞ assuming that ΔC_p is constant over the temperature range studied at 0.22 J g^{-1} K^{-1} based on the temperature dependence of ΔH_∞ at the three highest temperatures where values of $\Delta H_{a\infty}$ can be obtained. The value of ΔC_p is slightly smaller than that found from DSC cooling experiments ($= 0.25$ J g^{-1} K^{-1} at 97°C).

The values of the TNM model parameters found to fit the isothermal enthalpy recovery data are somewhat in agreement with the values cited in the literature [8]. The parameters obtained for isothermal enthalpy recovery are close to the literature values, with β within the range of values reported (0.55–0.80), Δh/R on the high side of the range reported (53–110 kK), and x on the low side of the reported values (0.44–0.52) [8].

3.4. Comparison of volume and enthalpy recovery

3.4.1. Time scales

We are now interested in comparing the time scales for volume and enthalpy recovery. However, the time required to reach equilibrium at a specific aging temperature is difficult to assess due to the asymptotic approach to equilibrium. In previous work, we determined the time required to reach equilibrium by visual inspection [11,12]. Here, we fit the data to the stretched exponential function:

$$\delta = \delta_0 \exp\left\{-\left(\frac{t}{\tau_{ch}}\right)^{\beta}\right\} \tag{6}$$

The nonexponential parameter β and the characteristic relaxation time τ_{ch} obtained from Eq. (6) do not have physical significance because the nonlinearity of the structural recovery process is not accounted for; i.e. Eq. (6) cannot describe the asymmetry of approach experiments [2]. The equation fits the data, however, because the nonexponential factor β compensates for neglecting the nonlinearity. Rearranging the stretched exponential function, we obtain the time required to reach equilibrium (t_∞):

$$t_\infty = \tau_{ch}\left[\ln\left(\frac{\delta_0}{\delta_\infty}\right)\right]^{1/\beta} \tag{7}$$

where δ_∞ is the value of δ at our arbitrary definition of equilibrium and δ_0 is used as a fitting parameter. The criteria we used for reaching equilibrium is $\delta_{\infty v} = 0.01 \times 10^{-3}$ and $\delta_{\infty h} = 0.01$ J/g. These criteria are equivalent since the initial departure from equilibrium at 97°C for volume is approximately one thousandth of that for enthalpy: $\delta_{0,v} =$

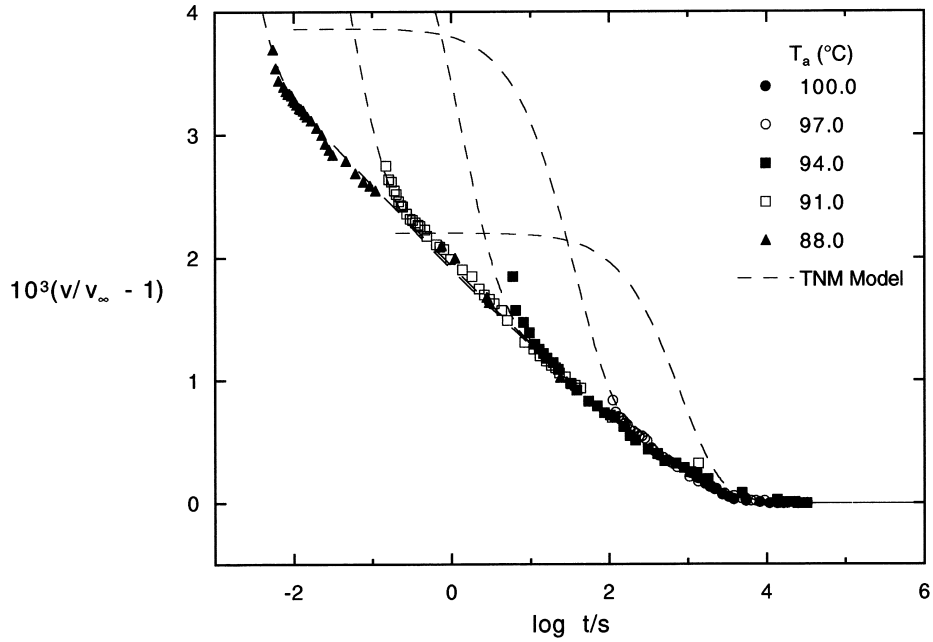

Fig. 6. Time–temperature superposition of the relative departure from equilibrium for volume. Lines are the fit to the TNM model of structural recovery, shifted separately for best superposition near equilibrium.

1.4×10^{-3} and $\delta_{0,h} = 1.1$ J/g. (Taking $\delta_{\infty h} = 0.008$ since $\delta_{0,h} = 800\ \delta_{0,v}$ made no significant difference in t_∞.)

Fig. 5 shows the time required to reach equilibrium for both volume and the enthalpy recovery as a function of temperature as determined by the criteria above using Eq. (7), as well as the times required to reach equilibrium (defined by the same criteria) calculated for all temperatures from the fit of the TNM structural recovery model. We also plot the shift factors, $\log a_T$, which will be discussed later. For now, we focus on the times required to reach equilibrium. The agreement is good between the model calculations and the stretched exponential, although not perfect since the model was fit to all five temperatures simultaneously, whereas the stretched exponential fits were performed separately for each aging temperature where equilibrium was attained. The error bars in the times required to reach equilibrium for enthalpy data are related to the scatter in the data which results in uncertainty in ΔH_∞. The error bars were obtained by fitting the data with the stretched exponential function using $\Delta H_\infty \pm$ one standard error to obtain the upper and lower limits of t_∞. We suggest that the data indicate that the times required to reach equilibrium are the same for volume and enthalpy recovery for the temperatures between 94 and 100°C where equilibrium was achieved in the experimental data.

On the other hand, the model predictions of the times required to reach equilibrium indicate that the equilibrium times diverge below about 94°C due to a difference in the apparent activation energies for volume and enthalpy recovery. The apparent normalized activation energies (Δh/R) for volume and enthalpy from the times required to reach equilibrium from the TNM calculations were obtained from Arrhenius plots and are 157 and 101 kK. From the TNM model itself, values of 146 and 100 kK were obtained for the apparent activation energy (Δh/R). The slightly higher value obtained from the times required to reach equilibrium from the model fits is attributed to the use of an arbitrary definition of equilibrium; the smaller δ_∞ is, the lower the difference between the activation energy obtained from the times to reach equilibrium and that used in the model calculations. Whether the difference in the activation energies for volume and enthalpy recovery is real or an artifact of problems with the TNM model [8,35,50–59] cannot be determined. It is clear, however, that extrapolation of the times required to reach equilibrium using the TNM model indicates that the equilibration times for volume and enthalpy will diverge at temperatures below those where equilibrium was achieved in the time scale of the experiments.

3.4.2. Shift factors

Another approach to approximating the temperature dependence of the times to reach equilibrium for data in which equilibrium is not attainable in experimental time scales is to examine the times required to reach a specified departure from equilibrium near equilibrium. We suggest that because the δ versus log time data appear to be approximately parallel at long times, the temperature dependence of the time required to reach equilibrium and that of the time required to reach a specified δ for small δ should be approximately the same. In other words, we propose that time–temperature superposition is valid at long times (small δs) and that we can obtain equilibrium shift factors from

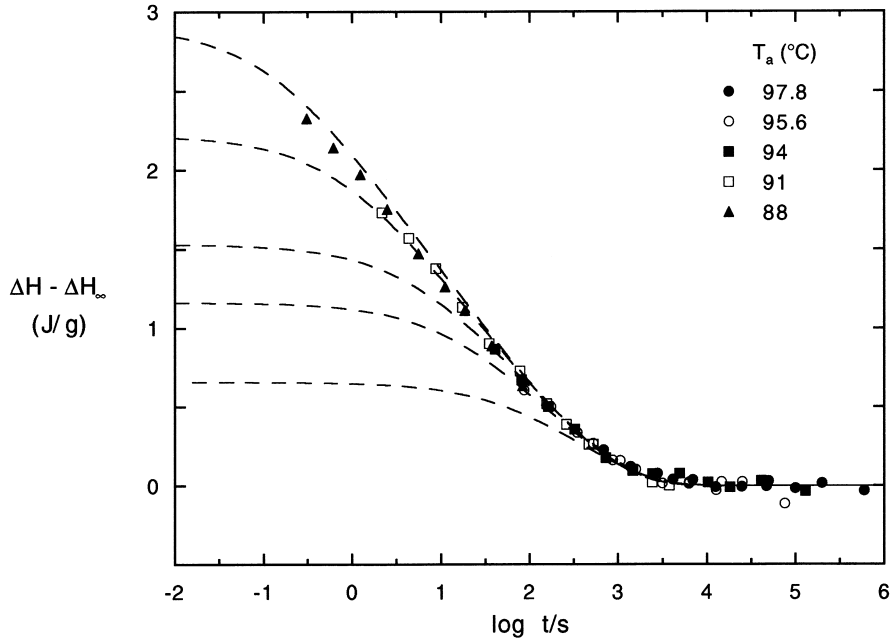

Fig. 7. Time–temperature superposition of the relative departure from equilibrium for enthalpy. Lines are the fit to the TNM model of structural recovery, shifted separately for best superposition near equilibrium.

reduction of the curves at long times. The error introduced by the shifting procedure has been quantified by a parametric analysis and is found to be vary from 0 to 10 kK at $\beta = 1.0$ depending on the value of x; as β decreases, the error increases to a maximum of 25 kK at $\beta = 0.2$ [41]. For a nominal set of parameters, $x = 0.4$, $\beta = 0.5$ and $\Delta h/R = 100$ kK, the error in $\Delta h/R$ estimated from the shift procedure is 10% [41]. This error is the same order of magnitude as that reported for fitting DSC curves [54]. The fact that the time required to reach equilibrium has the same temperature dependence as the shift factors (as will be shown shortly) also lends credence to the procedure. Obviously, one need not shift the curves to estimate the time to reach equilibrium or the apparent activation energy if one has fit the data to a

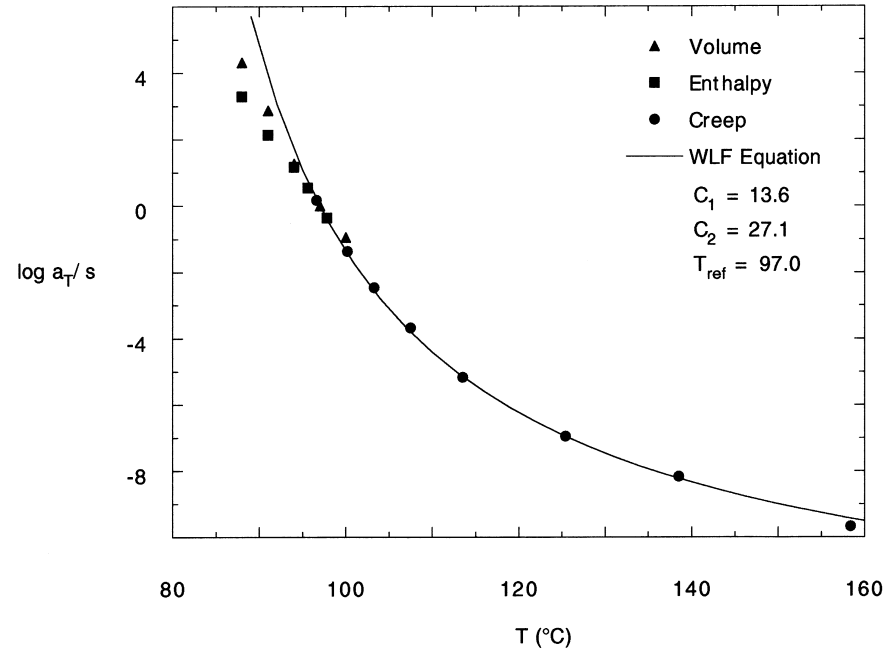

Fig. 8. WLF behavior of shift factors from reduction of volume and enthalpy data and from equilibrium creep recovery measurements Ref. [61], all for Dylene 8.

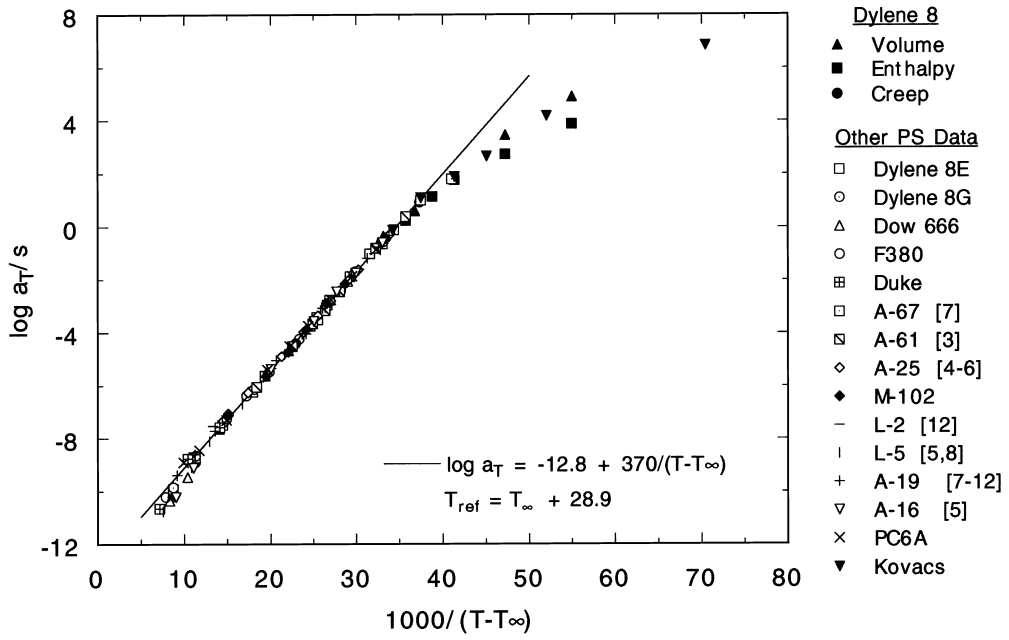

Fig. 9. VTHF plot of shift factors used to reduce volume, enthalpy, and creep data for Dylene 8 and other polystyrenes Refs. [45,60,64–67]. Polymer characteristics are listed in Table 3.

model of structural recovery since these values can be obtained from the model. However, the shifting procedure is simple and gives in most instances a reasonable approximation of $\Delta h/R$.

Fig. 6 shows the result of shifting the volume data horizontally to the reference temperature of 97°C in such a way that the data superpose at long times. The dashed lines are the model calculations (with the temperature quench included) presented in Fig. 2 and they are shifted separately to also give the best superposition at long times. Data superpose only at long times for small δs. Data deviate from the common asymptote to approach $\delta_0 = (v_0 - v_\infty)/v_\infty$ at short times.

The enthalpy data shown in Fig. 4 are analyzed in an analogous manner in Fig. 7. The model calculations are shown by the dashed lines and are shifted independently to give the best superposition at long times. Here again, data coincide to a reduced curve only at long times for small δs.

The shift factors, $\log a_T$, used to shift the volume and enthalpy data and the volume and enthalpy model calculations are shown in Fig. 5. The shift factors obtained from shifting the data and from shifting the model curves are very similar as expected since the model describes the data well. The shift factors appear to be nearly the same for the two properties at temperatures above approximately 94°C. Below 94°C, the shift factors diverge. The apparent normalized activation energies, obtained from Arrhenius plots (not shown), are 142 and 112 kK for volume and enthalpy, respectively. The temperature dependence is in agreement with $\Delta h/R$ obtained from the model fits (147 and 100 kK, respectively) and also agrees with the temperature

Table 3
Material characteristics for polystyrenes used in Fig. 9

Material or ID code	M (kg/mol)[a]	PDI	T_∞ (°C)	T_g[b] − T_∞ (°C)
Commercial samples				
Dylene 8 [61]	92.8	2.4	69.8	27.1
Dylene 8E [61]	104.0	2.5	69.9	27.l
Dylene 8G [61]	122.0	2.4	70.0	27.2
Dow 666 U-26 [61]	104.0	2.5	65.2	31.8
F380 [65]	3840	1.05	69.5	28.5
Duke standard [65]	7100	1.1	70.0	28.0
Fractionated samples				
A-67 [7][c] [66]	1.1	1.03	5.8	34.2[d]
A-61 [3] [66]	16.4	–	65.0	26.8
A-25 [4–6] [66]	46.9	1.05	67.5	28.3
M-102 [66]	94	<1.08	68.0[e]	28.9
L-5 [5,8] [66]	122	1.05	67.6	29.6
L-2 [12] [66]	189	1.01	70.0	27.5
A-19 [7–12] [66]	592	1.06	70.0	27.8
A-16 [5] [66]	800	–	69.5	28.4
PC6A [66]	773	<1.12	69.0	28.9
Kovacs [45]	400	–	69.7	28.0
Average				28.6
Standard deviation				1.9

[a] Number-average molecular weight except for fractionated samples which are viscosity-average molecular weights for Ref. [38] and weight-average molecular weight for Ref. [40].
[b] $T_g = 98.0–1.02 \times 10^5/M$ as determined by Altares [65].
[c] Bracketed numbers denote fractions.
[d] Using $T_g = 40$°C, the value estimated by DSC [65].
[e] Used to fix other relative values due to the large temperature range over which data was taken.

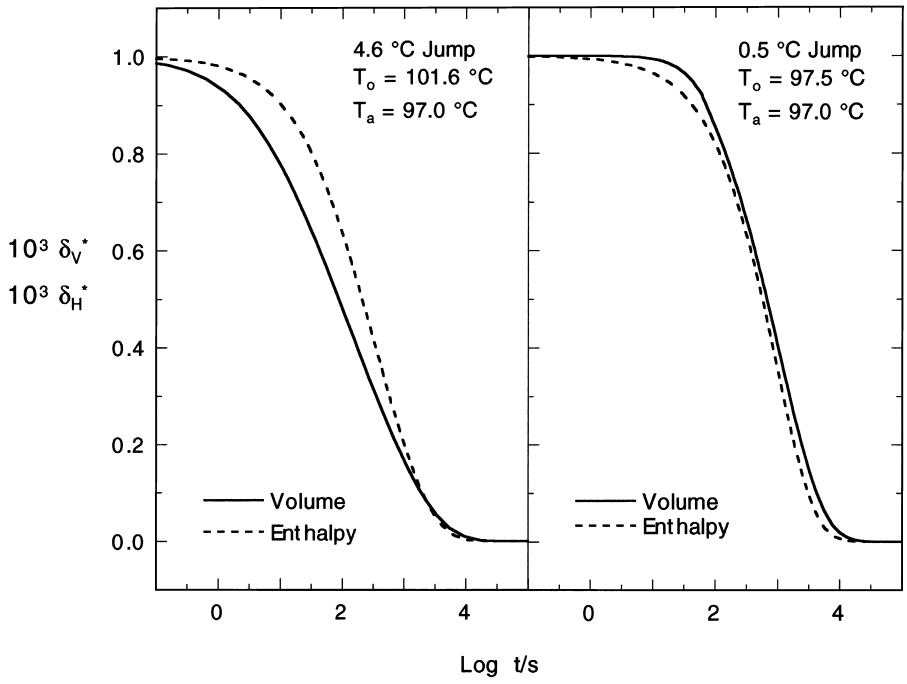

Fig. 10. Comparison of normalized volume and enthalpy recovery at 97°C predicted from model calculations, for temperature jumps of 4.6 and 0.5°C, respectively.

dependence of the times required to reach equilibrium obtained from the time to reach equilibrium results (157 and 101 kK, respectively.)

3.4.3. Temperature dependence of equilibrium below T_g

We indicated above that the times required to reach equilibrium and the shift factors obtained from our shifting procedure appear to have an Arrhenius temperature dependence. This is not unexpected given the limited 12°C temperature range over which data are taken. In Fig. 8, we show the shift factor data from volume and enthalpy recovery, along with shift factors obtained from creep/recovery measurements [60] in the softening dispersion for the same polystyrene. The creep data show the expected WLF (William–Landel–Ferry) [32] behavior. We note that the creep shift factor at the highest temperature examined (>180°C) is not shown in this figure (it is shown in Fig. 9) because its temperature dependence is that of the terminal zone rather than the softening dispersion. Fig. 8 indicates that the shift factors at the lowest aging temperatures studied deviate from the WLF behavior.

In Fig. 9, we show the equivalent Vogel [61]–Tammann–Hesse [62]–Fulcher [63] (VTHF) plot of the shift factors versus the reciprocal of $(T - T_\infty)$, where T_∞ is a constant which is approximately 29°C below T_g. In this figure, we compare not only the shift factors found in this work and those for equilibrium creep measurements for Dylene 8 [60] but also creep data for various polystyrenes including other commercial samples [60,64] and fractionated samples [65,66], as well as shift factors reported by Braun and Kovacs [45] for volume recovery data. The values of the parameter T_∞ used for the reduction of the data are shown in Table 3; the values are consistent with those found previously [60]: we find $(T_g - T_\infty) = 28.6$ with a standard deviation of 1.9°C. Similar to the WLF plot, the VTHF temperature dependence appears to be valid over a wide temperature range for the various polystyrenes tested, but it does not fit data from this work and from that of Kovacs [45] for temperatures below the glass temperature where the temperature dependence appears to be significantly weaker. Far above the glass temperature, also, the temperature dependence decreases and becomes Arrhenius; this latter fact is better well-known.

The deviation from the WLF or Vogel temperature dependence for the characteristic relaxation time at equilibrium density below T_g is not well-known or accepted. The most convincing data depicting the change from WLF to Arrhenius temperature dependence at T_g is the recent work on polycarbonate by O'Connell and McKenna in which equilibrium was reached at temperatures 17°C below the nominal glass temperature [67]. These results are consistent with the results of earlier researchers, although the observation that the change from WLF to Arrhenius temperature dependence appears to occur at T_g is new. For example, Plazek showed nearly twenty years ago that the temperature shift factors from creep data could not be fit by the same Vogel equation presumably because of the presence of two dispersions with different temperature dependences [68]. More recently, Stickel, Fischer and Richert suggested that all glass-forming materials exhibit two temperature

regimes, each describable by the Vogel equation in addition to a third Arrhenius regime at high temperatures [69]. Early work on B_2O_3 by Macedo and Napolitano [70], shows two Vogel temperature dependencies, but the change in temperature dependence from one Vogel equation to the other occurs several hundred degrees above T_g. However, recent data on B_2O_3 from our laboratory [71], which was analyzed along with the data of Macedo and Napolitano, suggests that the viscosity of B_2O_3 departs from the Vogel temperature dependence in the vicinity T_g. Similar behavior might be interpreted from earlier works on various organic liquids [72,73], but it is not clear in those works that the measurements reported are all made at equilibrium density. Finally we note that recent theoretical work by Di Marzio and Yang predicts a change in the temperature dependence of the equilibrium relaxation time at T_g from WLF-type dependence to an Arrhenius temperature dependence [74]. The non-WLF temperature dependence below T_g for the equilibrium state has major implications for modeling and predicting the effects of structural recovery, especially for aging deep in the glassy state, since knowledge of the value of the relaxation time at equilibrium is critical for accurate predictions.

3.4.4. Approach to equilibrium

Finally, it is of interest to examine the relative rates of approach to equilibrium for volume and enthalpy recovery. To this end, Fig. 10 shows the normalized volume and enthalpy recovery at 97°C calculated from the TNM model using the best fit parameters for volume and enthalpy, respectively. The normalization procedure is such that the data go from 1.0 initially to 0.0 at equilibrium. The calculations are for two perfect temperature jumps, one from 101.6 to 97.0°C, and the other for a more linear jump from 97.5 to 97.0°C. It is obvious that the approach to equilibrium for volume and enthalpy differ for the 4.6°C jump, indicating that their sensitivities to the underlying structural change that occurs during structural recovery differ. This is similar to the result found for poly(ether imide) [12]. However, it is interesting to note that as the jump becomes more linear, the differences between the two responses vanish. Mathematically, this is because the TNM parameter β is essentially the same for volume and enthalpy, whereas the nonlinearity parameter x is significantly different. This suggests that the differences in approach to equilibrium that have been observed for volume and enthalpy recovery may only be due to the nonlinearity of the process, rather than to inherent differences between the two processes.

The observations reported in this work, that volume and enthalpy recovery data come to equilibrium at the same time (for temperatures above approximately 94°C) although they do not have the same approach to equilibrium, are similar to those observed by us previously for polyetherimide [11,12]. Our results on relative time scales of volume and enthalpy recovery of polystyrene are consistent with the work of Oleinik [23], who reported that dH/dV is a constant during aging — we observe the same except very near to equilibrium. The results are also not inconsistent with those of Adachi and Kotaka [13] and Weitz and Wunderlich [14], both of whom reported on aspects of the relative kinetics of volume and enthalpy recovery. However, we argue that differences in the kinetics of volume and enthalpy recovery should not necessarily be interpreted to mean that volume and enthalpy recovery are decoupled. In fact, the two properties appear to come to equilibrium at the same time for the temperatures in which equilibrium was achieved in the time scale of the experiment. In addition the model predicts that the two properties will have the same normalized response in the limit of a linear temperature jump at 97.0°C. This indicates to us that the properties are not decoupled. The fact that the TNM model apparent activation energies differ does, however, argue against our interpretation of the data or the model's validity and, in either case, suggests a need for further investigations.

The results in this work do not necessarily address the relative evolution of mechanical properties and thermodynamic properties, in which differences in time scales have also been observed [16,17,19–22]. The apparent lack of universality of those results may also be a reflection of the effect of differences in the nonlinearity of the structural recovery response for different properties.

4. Conclusions

Volume and enthalpy recovery measurements have been used to study the physical aging behavior of a polystyrene in the vicinity of the glass temperature. Data are well-described by the TNM model of structural recovery. The times required to reach equilibrium, as well the shift factors used to shift the data such that they superpose at long times (at small δs), are identical for the two properties for temperatures above 94°C where data came to equilibrium during the experiments. The shift factors and the TNM model predict that at lower temperatures, where we were not able to achieve equilibrium due to the long time scales involved, the times required to equilibrium would diverge for the two properties. The shift factors used for the reduction of the data have a temperature dependence which is weaker than the WLF or VTHF temperature dependence which described equilibrium creep shift factor data obtained in other work. In addition, the rate of approach to equilibrium for volume and enthalpy was examined. For nonlinear jumps, the normalized responses at 97°C differed. However, as the jumps became more linear, the normalized responses became almost identical. We suggest that this indicates that the effective relaxation time spectrum for the two properties is similar, but that the nonlinearity of the structural recovery response for volume and enthalpy differ.

Acknowledgements

The authors would like to acknowledge the helpful discussions with Dr Gregory B. McKenna of the Department of Chemical Engineering at Texas Tech University, as well as the work of Lily Giri, Lei Zhang, and Elliot Wolf in obtaining the volume and enthalpy data. S.L.S. acknowledges partial support from American Chemical Society Petroleum Research Foundation (32555 AC7) and both D.J.P. and S.L.S. acknowledge partial support from the National Science Foundation DMR 9530372.

References

[1] Struik LCE. Physical aging in amorphous polymers and other materials. New York: Elsevier, 1978.
[2] Kovacs AJ. Adv Polym Sci 1963;3(3):394.
[3] Cowie JMG. J Macromol Sci, Phys 1980;B18(4):569.
[4] Plazek DJ, Berry GC. Glass: Sci Tech 1986;3:363.
[5] O'Reilly J. CRC Crit Rev Solid State Mater Sci 1987;13(3):259.
[6] McKenna GB. In: Booth C, Price C, editors. Comprehensive polymer science, Polymer properties, Vol. 2. Oxford: Pergamon, 1989 (chap. 2).
[7] Scherer GW. J Non-Cryst Solids 1990;123:75.
[8] Hodge I. J Non-Cryst Solids 1994;169:211.
[9] Mijovic J. Polym Engng Sci 1994;34:381.
[10] Hutchinson JM. Prog Polym Sci 1995;20:703.
[11] Echeverria I, Su P-C, Simon SL, Plazek DJ. J Polym Sci, Part B: Polym Phys 1995;33:2457.
[12] Simon SL, Plazek DJ, Sobieski JW, McGregor ET. J Polym Sci, Part B: Polym Phys 1997;35:929.
[13] Adachi K, Kotaka T. Polym J 1982;14:959.
[14] Weitz A, Wunderlich B. J Polym Sci, Polym Phys Ed 1974;12:2473.
[15] Roe RJ, Millman GM. Polym Engng Sci 1983;23:318.
[16] Petrie SEB. In: Allen G, Petrie SEB, editors. Physical structure of the amorphous state. New York: Marcel Dekker, 1975.
[17] Sasabe H, Moynihan CT. J Polym Sci, Part B: Polym Phys 1978;16:1447.
[18] Cowie JMG, Elliott S, Ferguson R, Simha R. Polym Commun 1987;28:298.
[19] Perez J, Cavaille JY, Calleja RD, Ribelles JLG, Pradas MM, Greus AR. Makromol Chem 1991;192:2141.
[20] Mijovic J, Ho T. Polymer 1993;34:3865.
[21] McKenna GB, Schultheisz CR, Leterrier Y, Deformation yield and fracture of polymers. In Proceedings of the Ninth International Conference, Cambridge, UK, 1994. p. 31/1–31/4.
[22] McKenna GB, et al. Polym Engng Sci 1995;35(5):403.
[23] Oleinik EF. Polym J 1987;19(1):105.
[24] Bero CA, Plazek PJ. J Polym Sci, Part B: Polym Phys 1991;29:39.
[25] McKenna GB, Hutchinson JM (discussion leaders). Third International Discussion Meeting on Relaxations in Complex Systems, June 30–July 11, 1997, Vigo Spain.
[26] Moynihan CT, Macedo PB, Montrose CJ, Gupta PK, DeBolt MA, Dill JF, Dom BE, Drake PW, Esteal AJ, Elterman PB, Moeller RP, Sasabe H, Wilder JA. Ann NY Acad Sci 1976;15:279.
[27] Narayanaswamy OS. J Am Ceram Soc 1971;54:491.
[28] Tool AQ. J Am Ceram Soc 1946;29:240.
[29] Kovacs AJ, Aklonis JJ, Hutchinson JM, Ramos AR. J Polym Sci, Polym Phys Ed 1979;17:1097.
[30] Kolrausch F. Pogg Ann Phys 1847;12:393.
[31] Williams G, Watts DC. Trans Faraday Soc 1970;66:80.
[32] Williams ML, Landell RF, Ferry JD. J Am Chem Soc 1955;77:3701.
[33] Boltzmann L. Wied Ann 1878;5:430.
[34] Hodge IM, Berens AR. Macromolecules 1982;15:762.
[35] Simon SL. Macromolecules 1997;30:4056.
[36] Simon SL, McKenna GB. J Chem Phys 1997;107(20):8678.
[37] Simon SL, McKenna GB. Thermochim Acta 1997;307:1.
[38] Santore MM, Duran RS, McKenna GB. Polymer 1991;32(13):2377.
[39] Struik LCE. Polymer 1987;28:1869.
[40] Struik LCE. Polymer 1997;38(18):4677.
[41] Sobieski JW. PhD thesis. University of Pittsburgh, December 1999.
[42] Menczel JD, Leslie TM. Thermochim Acta 1990;166:309.
[43] Hutchinsons JM, Ruddy M, Wilson MR. Polymer 1988;29:152.
[44] Kuester JL, Mize JH. Optimzation techniques with Fortran. New York: McGraw Hill, 1973.
[45] Braun G, Kovacs AJ. Phys Chem Glasses 1963;4(4):152.
[46] Greiner R, Schwarzl FR. Rheol Acta 1984;23:378.
[47] Lee HH-D, McGarry FJ. Polymer 1993;34(20):4267.
[48] Ueberreiter K, Kanig G. J Colloid Sci 1953;7:569.
[49] McKinney JE, Simha R. J Res Nat Bur Stand: A Phys Chem 1977;81A(2–3):283.
[50] Moynihan CT, Crichton SN, Opalka SM. J Non-Cryst Solids 1991;131–133:420.
[51] Moynihan CT. Rev Miner 1995;32:1.
[52] McKenna GB, Angell CA. J Non-Cryst Solids 1991;133-133:528.
[53] Scherer GW. J Am Ceram Soc 1986;69(5):374.
[54] Hodge IM, Huvard GS. Macromolecules 1983;16:371.
[55] Tribone JJ, O'Reilly JM, Greener J. J Polym Sci, Part B: Polym Phys 1989;27:37.
[56] O'Reilly JM, Hodge IM. J Non-Cryst Solids 1991;131–133:451.
[57] Medvedev G, Caruthers JM. Society of Rheology, Madison, WI, October 17–21, 1999.
[58] McWilliams D. PhD thesis. Purdue University, 1999.
[59] Rekhson S, Ducroux J-P. In: Pye LD, La Course WC, Stevens HJ, editors. The physics of non-crystalline solids. London: Taylor and Francis, 1992. p. 315.
[60] Agarwal PK. PhD thesis. University of Pittsburgh, 1975.
[61] Vogel H. Phys Z 1921;22:645.
[62] Tammann G, Hesse G. Z Anorg Allg Chem 1926;156:245.
[63] Fulcher GS. J Am Chem Soc 1925;8:339 see also 789.
[64] Plazek DJ. Unpublished data.
[65] Plazek DJ, O'Rourke VM. J Polym Sci, Part A-2 1971;9:209.
[66] Riande E, Markovitz H, Plazek DJ, Raghupathi N. J Polym Sci, Polym Symp 1975;50:405.
[67] O'Connell PA, McKenna GB. J Chem Phys 1999;110(22):11054.
[68] Plazek DJ. J Polym Sci, Polym Phys Ed 1982;20:729.
[69] Stickel F, Fischer E, Richert R. J Chem Phys 1996;104:2043.
[70] Macedo, Napolitano. J Chem Phys 1968;49(4):1887.
[71] Bernatz K. PhD thesis. University of Pittsburgh, 1999.
[72] Laughlin WT, Uhlmann DR. J Phys Chem 1972;76:2317.
[73] Cukierman M, Lane JW, Uhlmann DR. J Chem Phys 1973;59:3639.
[74] Di Marzio EA, Yang AJM. J Res Nat Inst Stand Tech 1997;102(2):135.